Contribution of aroma precursors to the formation of aroma-active compounds in hot-air-dried shrimp studied by reaction models

ZEWEI ZHANG – HONGWU JI – DI ZHANG – SHUCHENG LIU – XIAOSHAN ZHENG – WEIZHEN SUN

Summary
Aroma-active compounds in dried shrimp were investigated by aroma extract dilution analysis. Amino acids (Lys, Arg, Phe, Leu and Ile), reducing sugars (glucose, galactose, and arabinose) and total lipids were selected as precursors to construct 23 models, and then reacted at temperatures consistent with shrimp drying. The formation status and content of dried shrimp aroma-active compounds in each model were examined using gas chromatography-mass spectrometry. Twenty-seven aroma-active compounds were identified in the dried shrimp with flavour dilution (*FD*) factor ranges of 3 to 729, including 13 pyrazines, 5 aldehydes, 5 ketones, 2 alcohols and 2 N-containing compounds. Among them, *FD* factors of 5 pyrazines and trimethylamine were greater than 243. Pyrazines were the most important class of aroma-active compounds. The results of reaction model application indicated that Lys and Arg were the primary amino precursors of 13 aroma-active pyrazines and trimethylamine. Phe, Leu and Ile formed benzaldehyde, 3-methylbutanal and 2-methylbutanal, respectively. Glucose was the main carbonyl precursor. Lipids were the precursors of 2 alkylaldehydes, 4 ketones and 1-octen-3-ol, promoting the formation of pyrazines and Strecker aldehydes. This study provides a reference for improving flavour production and regulation of dried shrimp products, in particular the shrimp seasoning.

Keywords
dried shrimp; aroma precursors; aroma-active compounds; reaction model; aroma extract dilution analysis; gas chromatography-olfactometry

Penaeus vannamei is one the most notable farmed shrimp species in China, which is a global leader in shrimp production [1]. Shrimp spoilage occurs rapidly after capturing due to the delicate tissue structure, the substantial microbiological load of fresh shrimps and the high moisture content. Therefore, preservation methods must be employed [2]. Drying is one of the best methods for preserving shrimp, with a long history and mature technology. The uniquely pleasant aroma and extended shelf-life are the main attractions for customers [3]. The aroma of dried shrimp is derived from a combination of volatile components. Gas chromatography-mass spectrometry (GC-MS) is the most widely used method for detecting the volatile compounds of dried shrimp [4]. Typically, aroma-active compounds (AAC) are volatile compounds with an odour activity value (*OAV*) greater than 1, where *OAV* is the ratio of their content to the odour threshold values [5]. AAC in hot air-dried shrimp was found to include mainly 3-ethyl-2,5-dimethylpyrazine, 2-ethyl-5-methylpyrazine, 2,5-dimethylpyrazine, 2-acetyl-1-pyrroline, 1-octen-3-ol, benzaldehyde, 3-methylbutyraldehyde,

Zewei Zhang, Hongwu Ji, Di Zhang, Xiaoshan Zheng, Weizhen Sun, College of Food Science and Technology, Guangdong Ocean University; Guangdong Provincial Key Laboratory of Aquatic Products Processing and Safety; Guangdong Province Engineering Laboratory for Marine Biological Products; Guangdong Provincial Engineering Technology Research Center of Seafood; Key Laboratory of Advanced Processing of Aquatic Product of Guangdong Higher Education Institution, No. 1 Haida Road, Mazhang, Zhanjiang 524088, China.
Shucheng Liu, College of Food Science and Technology, Guangdong Ocean University; Guangdong Provincial Key Laboratory of Aquatic Products Processing and Safety; Guangdong Province Engineering Laboratory for Marine Biological Products; Guangdong Provincial Engineering Technology Research Center of Seafood; Key Laboratory of Advanced Processing of Aquatic Product of Guangdong Higher Education Institution, No. 1 Haida Road, Mazhang, Zhanjiang 524088, China; Collaborative Innovation Center of Seafood Deep Processing, Dalian Polytechnic University, No. 1 Qinggongyuan, Ganjingzi District, Dalian 116034, China.

Correspondence author:
Hongwu Ji, e-mail: Jihw62318@163.com

2-methylbutyraldehyde and trimethylamine [6]. However, it is impractical to obtain the threshold values for each volatile compound. That method also neglects the sensory properties of the samples and cannot accurately determine the impact of a single AAC on the overall sensory experience of dried shrimp. The gas chromatography-olfactometry (GC-O) technique is a powerful analytical method that combines GC with an olfactometer to analyse volatile compounds in samples, leveraging the strengths of both instrumental precision and human senses [7]. The GC-O analytical method can precisely investigate the contribution of a single AAC to the overall sample's odour. Aroma extract dilution analysis (AEDA) is an odour analysis method used with GC-O, which can effectively screen and identify AAC in food [8]. It has been applied in rice, fish, fruit, beef and mushroom [9], but less research has been done regarding AAC of dried shrimp.

AAC in dried shrimp are primarily generated by the Maillard reaction, lipid oxidation, and lipid-Maillard interaction reaction during drying [10]. During the thermal processing of food, lipid oxidation and Maillard reaction coincide. Their reaction courses can be modified by varying the reactants, intermediates and products to generate diverse AAC. Various aroma precursors in raw shrimp, including various amino acids, reducing sugars and lipids, can participate in these reactions. Targeted regulation of the formation of AAC in dried shrimp could help optimize and understand the process, improve the quality and provide the reference for production technology [11]. However, due to the diversity of aroma precursors and the complexity of the reaction pathways, it is challenging to target and regulate the formation of AAC in dried shrimp. In order to effectively regulate the formation of AAC, it is necessary to study the correlation between aroma precursors and AAC of dried shrimp, whether the component is an aroma precursor or plays a role in promoting AAC formation. Previous research compared the variations in AAC types and contents in dried shrimp when either amino acids were added to raw shrimp [6], or lipids removed [12]. Results of those studies showed that amino acids (Lys, Arg, Phe, Leu and Ile) and lipids had significant impact on AAC formation in the hot-air-dried shrimp. Additionally, some AAC were influenced by multiple precursors, with Lys, Arg and lipids contributing significantly to the formation of pyrazines. However, correlations with AAC formation in dried shrimp have not been systematically investigated and reported.

The generation of food aroma is highly complex, so it is difficult to determine precisely the correlation between aroma precursors and AAC. Developing a thermal reaction model or isotopic model to investigate these complex and interrelated reaction pathways was used previously [13]. Isotopic model studies investigated the formation pathways of crucial aroma compounds in meat aroma [14, 15]. However, there are many precursor substances involved in food aroma formation. The isotopic model is challenged to label each precursor and is expensive. Building a thermal response model system seems a more effective choice. A Maillard reaction system model has been widely used to investigate the relationship between amino acids, sugars and volatile compounds such as pyrazine formation [16, 17]. However, developing reaction systems to track the contribution of aroma precursors to the formation of AAC within the hot-air-dried shrimp has not yet been reported.

The study firstly aimed to determine the AAC in dried shrimp using AEDA. Secondly, a reaction model system was constructed considering combinations of amino acids (Lys, Arg, Phe, Leu and Ile), reducing sugars (D-glucose, D-galactose and D-arabinose) and lipids. The formation status and content of AAC in dried shrimp in each model were examined using GC-MS. Finally, the relationship between aroma precursors and AAC of dried shrimp was intuitively analysed.

MATERIALS AND METHODS

Chemicals

L-Lys, L-Arg, L-Phe, L-Leu and L-Ile (biological reagent grade) and 2-ethyl-3,6-dimethylpyrazine (GC grade, ≥97.0 %) were obtained from Shanghai Yuanye Bio-Technology (Shanghai, China). D-glucose (GLU), D-galactose (GAL) and D-arabinose (ARA; all biological reagent grade), 3-methylbutanal (GC grade, ≥98.0 %) and pentanal (GC grade, ≥98.0 %) were from Shanghai Macklin Biochemical Technology (Shanghai, China). Chloroform and methanol (analytical grade) were obtained from Xilong Scientific (Shantou, China). Nonanoic acid methyl ester (GC grade, ≥99.0 %), 2-ethyl-5-methylpyrazine (GC grade, ≥98.0 %), 2,5-dimethylpyrazine (GC grade, ≥98.0 %), 2,3,5-trimethylpyrazine (GC grade, ≥99.0 %), 2,6-dimethylpyrazine (GC grade, ≥98.0 %), tetramethylpyrazine (GC grade, ≥98.0 %), 2,3-dimethylpyrazine (GC grade, ≥99.0 %), 2-acetyl-3-methylpyrazine (GC grade, ≥99.0 %), benzaldehyde (GC grade, ≥99.0 %), 2-octanone (GC grade, ≥98.0 %), 2-nonanone

(GC grade, ≥99.0 %), 1-octen-3-ol (GC grade, ≥98.0 %) and 2-acetyl-1-pyrroline (GC grade, ≥98.0 %) were obtained from Sigma-Aldrich Chemical (St. Louis, Missouri, USA).

Preparation of samples

The sample preparation was conducted according to the method of ZHANG et al. [18]. Fresh shrimps (*Penaeus vannamei*) with an average weight of 20.0 g were purchased at a local market in Zhanjiang City, Guangdong Province, China in August 2022. The well-blended raw shrimps were applied to the glass plate with a 1 mm thick coating. The glass plates were placed in an electric thermostatic blast furnace Eyela NDO-710 (Tokyo Rikakikai, Tokyo, Japan) with the internal temperature maintained at 85 °C. Samples with a moisture content of approximately 8 % were obtained, stored at –18 °C, and used within 3 days of preparation.

Total lipid extraction

Total lipid extraction was performed according to the method of FOLCH et al. [19]. An amount of 20 g of fresh shrimps were blended with 400 ml of chloroform-methanol (2 : 1, v/v) and then homogenized. The homogenate solution was kept at 4 °C for 24 h and then filtered through qualitative filter paper 102 (General Electric Biotechnology, Hangzhou, China). The filtrate was added to an equal volume of 0.03 mol·l^{-1} $MgCl_2$ solution, shaken and allowed to stand for 1 h for separation into aqueous and organic phases. The organic phases were withdrawn and concentrated by high-throughput vacuum parallel concentrator (RayKol Group, Xiamen, China) to obtain the total lipid (TL) fraction.

Construction of the reaction model

The reaction model was constructed according to the preparation method of hot-air drying shrimp [6]. Each reactant was mixed with 8.0 ml of phosphate buffer (0.2 mol·l^{-1}, pH 7.2) in a 40-ml bottle, which was then placed into an electric thermostat blast oven Eyela NDO-700 (Tokyo Rikakikai) at 85 °C for 5 h, followed by cooling in an ice bath for 3 min. The composition and the amounts of reactants added are shown in Tab. 1. The types of ami-

Tab. 1. Composition of models and added amounts of reactants.

Reaction model name			Lys	Arg	Phe	Leu	Ile	GLU	GAL	ARA	TL
			[g]								
Blank models	SAA	Lys	0.122	0	0	0	0	0	0	0	0
		Arg	0	0.136	0	0	0	0	0	0	0
		Phe	0	0	0.061	0	0	0	0	0	0
		Leu	0	0	0	0.123	0	0	0	0	0
		Ile	0	0	0	0	0.063	0	0	0	0
	SSU	GLU	0	0	0	0	0	0.014	0	0	0
		GAL	0	0	0	0	0	0	0.004	0	0
		ARA	0	0	0	0	0	0	0	0.008	0
	MAA		0.122	0.136	0.061	0.123	0.063	0	0	0	0
	MSU		0	0	0	0	0	0.012	0.004	0.008	0
	TL + MAA		0.122	0.136	0.061	0.123	0.063	0	0	0	0.181
	TL + MSU		0	0	0	0	0	0.012	0.004	0.008	0.181
Maillard reaction models	SAA + MSU	Lys + MSU	0.122	0	0	0	0	0.012	0.004	0.008	0
		Arg + MSU	0	0.136	0	0	0	0.012	0.004	0.008	0
		Phe + MSU	0	0	0.061	0	0	0.012	0.004	0.008	0
		Leu + MSU	0	0	0	0.123	0	0.012	0.004	0.008	0
		Ile + MSU	0	0	0	0	0.063	0.012	0.004	0.008	0
	SSU + MAA	GLU + MAA	0.122	0.136	0.061	0.123	0.063	0.012	0	0	0
		GAL + MAA	0.122	0.136	0.061	0.123	0.063	0	0.004	0	0
		ARA + MAA	0.122	0.136	0.061	0.123	0.063	0	0	0.008	0
	MAA + MSU		0.122	0.136	0.061	0.123	0.063	0.012	0.004	0.008	0
Lipid oxidation model	TL		0	0	0	0	0	0	0	0	0.181
Interaction reaction model	TL + MAA + MSU		0.122	0.136	0.061	0.123	0.063	0.012	0.004	0.008	0.181

SSA – single amino acid, SSU – single sugar, MAA – mixed amino acid, MSU – mixed sugar, TL – total lipid, GLU – D-glucose, GAL – D-galactose, ARA – D-arabinose.

no acids and sugars were identified by the method used in the previous studies [6]. The amounts of each reactant were added and the reaction pH was adjusted at the composition ratios and pH of the fresh shrimp samples, respectively.

HS-SPME-GC-MS analysis

Headspace solid-phase microextraction (HS-SPME) coupled to GC-MS of volatile compounds were performed according to ZHANG et al. [6]. A volume of 2 μl of the internal standard solution (nonanoic acid methyl ester, 0.0400 g·l^{-1} in methanol) was added to each sample. The bottle was sealed using a screw cap with a polytetrafluoroethylene-silicon spacer with a 50/30 μm divinylbenzene/carboxen/polydimethylsiloxane SPME needle inserted (1 cm, 50/30 μm; Supelco, Bellefonte, Pennsylvania, USA) with the fibre outstretched. The volatile compounds were then absorbed for 35 min while the water bath was maintained at 60 °C. The SPME needle was subsequently inserted into the injector port of the gas chromatograph to desorb volatiles at 240 °C for 5 min. The volatile compounds were detected by a TQ8050NX GC-MS system (Shimadzu, Tokyo, Japan). Separated was achieved using an Inert Cap Pure-Wax capillary column (30 m × 0.25 mm, 0.25 μm film thickness; Shimadzu). Helium (99.999% purity) was used as the carrier gas at a flow rate of 1.0 ml·min^{-1}. The heating programme of the column was as follows: 40 °C for 3 min; increase to 100 °C at a rate of 4 °C·min^{-1}; hold for 2 min; increase to 230 °C at a rate of 8 °C·min^{-1}; hold for 5 min. The temperature of the ion source was 230 °C and the electron ionization energy was 70 eV. Full scan mode was used across the *m*/*z* range of 33–550 amu.

GC-O analysis

An amount of 2.00 g dried shrimp sample was accurately weighed into a 40 ml headspace bottle. The extraction of odours by SPME and analysis conditions by GC-O-MS was the same as those described in the previous paragraph on HS-SPME-GC-MS. The end effluent from the capillary column flowed into the MS and olfactory detector OP275 Pro II (GL Sciences, Saitama, Japan) at a split ratio of 1 : 1. The temperature of the outlet of the olfactometer and transfer line were 230 °C and 250 °C, respectively. High-purity nitrogen (99.99 %; Zhanjiang Xiqiang Industrial Gas, Zhanjiang, China) was used as the auxiliary gas in the sniffing process.

Aroma extract dilution analysis

AEDA was performed based on the method of CHEN et al. [20], with appropriate improvements. The flavour dilution (*FD*) factor of each compound was determined. The dilution was achieved by adjusting the GC injection split ratio to 1 : 3n (n = 1, 2, … 9), yielding a maximum dilution factor of 729. The GC-O analysis was carried out by 3 well-trained panelists. Sniffing at all dilution levels was repeated twice and data were only recorded for aroma compounds perceived by at least two panelists at the same retention time. The *FD* factor of each compound represents the maximum dilution at which the odorant can be perceived.

Volatile compounds identification analysis

Identification of the volatile compounds was based on comparing the MS fragmentation pattern of each compound with that in the NIST05 (National Institute of Standards and Technology, Gaithersburg, Maryland, USA) and Wiley07 (Palisade Corporation, New York, New York, USA) databases, with a requirement of a match degree greater than 80 %, and based on comparing retention indices. Aroma compounds with *FD* factors greater than 27 were further identified by comparing their MS data with those of the corresponding standard compounds.

Volatile compounds quantification

The content of each volatile compound was determined by the ratio of the peak area to the internal standard peak area under comparable GC-MS conditions. The content of each volatile compound was calculated using the following Eq. 1 [6]:

$$C_i = \frac{A_i \times C_s}{A_s} \quad (1)$$

where C_i is the content of the volatile compound detected in the sample, A_i is the compound peak area, C_s is the content of nonanoic acid methyl ester and A_s is the peak area of nonanoic acid methyl ester.

On the basis of identification and semi-quantification, aroma compounds with *FD* factors greater than 27 were quantified using calibration curves constructed from the odourless matrix of dried shrimp with varying contents of standards [21]. Specifically, standard solutions of various concentrations (0.0050 g·l^{-1} to 0.2000 g·l^{-1}) were prepared in methanol and 2 μl of the standard solution was added to 2 g of odourless matrix along with nonanoic acid methyl ester (2 μl, 0.0400 g·l^{-1} in methanol). The peak areas of the standards and nonanoic acid methyl ester were obtained by HS-SPME-GC-MS as described previously. The standard curves were constructed by plotting the ratio of the peak area of the reference compound

to that of the internal standard against their content ratio. All analyses were conducted in triplicate.

Statistical analysis

All experiments were carried out in triplicate and the data were expressed as mean ± standard deviation. The mean values were compared via one-way analysis of variance (post hoc test according to Tukey, two-tailed) using SPSS 23 software (IBM, Armonk, New York, USA) to test the significance of the differences ($P < 0.05$).

RESULTS AND DISCUSSION

Aroma active compounds in dried shrimp

Contribution of various aroma-active compounds to the overall aroma of dried shrimp was analysed using AEDA. In general, compounds with high *FD* factors contribute more to the overall aroma characteristic of a sample. As shown in Tab. 2, 27 types of AAC were identified in the dried shrimp, including 13 pyrazines, 5 aldehydes, 5 ketones, 2 alcohols and 2 N-containing compounds. Most of these volatile compounds have been previously reported in several shrimp species [18, 22].

Among AAC, 6 compounds were found to have markedly higher *FD* values ($FD \geq 243$). These compounds contributed aroma notes described as roasted nutty (2-ethyl-3,6-dimethylpyrazine), coffee bean (2-ethyl-5-methylpyrazine), roasted cocoa (2,5-dimethylpyrazine), roasted (2,3,5-trimethylpyrazine), nutty (2,6-dimethylpyrazine) and fishy (trimethylamine). These compounds, as potent odourants, played a crucial role in the aroma of dried shrimp.

With *FD* values ranging from 27 to 81, 10 compounds made medium contribution to the overall aroma of dried shrimp. These compounds were 2,3-dimethylpyrazine, 2-acetyl-3-methylpyrazine, tetramethylpyrazine, 3-methylbutanal, benzaldehyde, pentanal, 2-octanone, 2-nonanone, 1-octen-3-ol and 2-acetyl-1-pyrroline. They may contribute to the overall aroma of dried shrimp, especially providing roasted nutty, coffee, chocolate, bitter almond, fruity, earthy, mushroom and popcorn notes.

The 16 volatile compounds with $FD \geq 27$ were identified as key aroma compounds of dried shrimp in subsequent recombination and omission experiments (data not shown). Further, 11 compounds with *FD* values of $1 \leq FD \leq 9$ were identified. Although their *FD* factor was low and probably had a relatively little effect on the aroma of dried shrimp, they may contribute to the complex background aroma with their green, caramellic, fruity and floral notes.

Pyrazines

Pyrazines, as a group of volatile heterocyclic nitrogen-containing compounds, are low-odour-threshold volatile compounds in dried shrimp products and are considered a crucial flavour compound in the constitution of the characteristic aroma of dried shrimp [23]. Thirteen pyrazines were detected by smell in dried shrimp using GC-O. They accounted for almost half of 27 AAC. Among them, the *FD* factors of 5 pyrazine AACs were greater than 243. Their characteristic sensory impacts were generally described as desirable and favourable baked, roasted and nutty flavours [24]. The dried shrimp was commonly described as possessing roasted nutty aroma and pyrazines were identified as crucial aroma-active compounds of dried shrimp [18]. The mechanism of pyrazine generation is understood, being proposed based on experimental studies and computational model chemical simulations [25]. The nitrogen atoms of the pyrazine backbone are all derived from amino compounds. However, there are differences in the type and content of amino acids in different food matrices, affecting the formation of pyrazines [6]. In this study, amino acids in the reaction model were added according to their contents in raw shrimp. The drying conditions of dried shrimp were simulated to track the actual effect of amino acids on the formation of aroma-active compounds in dried shrimp.

The single amino acid (SAA), single sugar (SSU), mixed sugar (MSU) and mixed amino acid (MAA) models did not contain any pyrazines (Tab. S1 in supplementary data), indicating that amino acids or sugars alone could not produce pyrazines. Pyrazines were all detected in the Maillard reaction models of single amino acid with mixed sugar (SAA + MSU), single sugar with mixed amino acids (SSU + MAA) and in mixed amino acids with mixed sugar (MAA + MSU) and their content is illustrated on Fig. 1A, 1B, 1C and 1E. They were produced by reactions between amino acids and sugars in Maillard reaction, specifically between thermally induced carbohydrate degradation products and Strecker products of amino acids [26].

In the SAA + MSU models (Fig. 1A, 1B), 13 pyrazine AAC were detected in both the Maillard reaction models of Lys with mixed sugar (Lys + MSU) and in Arg with mixed sugar (Arg + MSU) with total contents of 594 ± 25.7 $\mu g \cdot kg^{-1}$ and 594 ± 41.9 $\mu g \cdot kg^{-1}$, respec-

Tab. 2. Flavour dilution factors of aroma-active compounds in dried shrimp.

Aroma-active compound	Odour description	Retention index	*FD*	Identification methods	Calibration equations	R^2
Pyrazines						
2-Ethyl-3,6-dimethylpyrazine	Cocoa, roasted, nutty	1412	729	MS, RI, O, S	$y = 0.5594x + 0.8863$	0.9926
2-Ethyl-5-methylpyrazine	Coffee, nutty	1358	729	MS, RI, O, S	$y = 0.0261x + 0.3798$	0.9662
2,5-Dimethylpyrazine	Cocoa, roasted	1292	729	MS, RI, O, S	$y = 1.0085x + 1.9241$	0.9885
2,3,5-Trimethylpyrazine	Nutty, roasted	1371	243	MS, RI, O, S	$y = 0.0898x + 0.3113$	0.9935
2,6-Dimethylpyrazine	Nutty, hazelnut	1295	243	MS, RI, O, S	$y = 0.0375x + 0.2781$	0.9699
Tetramethylpyrazine	Nutty, chocolate, cocoa	1457	81	MS, RI, O, S	$y = 0.7871x + 3.0833$	0.9792
2,3-Dimethylpyrazine	Coffee, nutty	1335	81	MS, RI, O, S	$y = 0.2715x + 0.1618$	0.9896
2-Acetyl-3-methylpyrazine	Roasted, nutty	1640	27	MS, RI, O, S	$y = 0.2000x + 0.3498$	0.9885
2-Acetylpyrazine	Roasted, nutty	1599	9	MS, RI, O	–	–
2,5-Dimethyl-3-(2-methylbutyl)pyrazine	Hazelnut, roasted	1576	9	MS, RI, O	–	–
2,6-Diethylpyrazine	Nutty, roasted	1295	3	MS, RI, O	–	–
2-Methylpyrazine	Nutty, roasted	1248	3	MS, RI, O	–	–
2,5-Dimethyl-3-propylpyrazine	Nutty, hazelnut	1525	3	MS, RI, O	–	–
Aldehydes						
3-Methylbutanal	Chocolate, fatty	876	81	MS, RI, O, S	$y = 0.0379x + 0.3262$	0.9887
Benzaldehyde	Bitter almond, cherry	1477	81	MS, RI, O, S	$y = 0.1717x + 0.3417$	0.9820
Pentanal	Fermented, fruity	976	81	MS, RI, O, S	$y = 0.0673x + 0.5948$	0.9906
2-Methylbutanal	Leather, smoke	913	3	MS, RI, O	–	–
Hexanal	Fresh, green	1183	3	MS, RI, O	–	–
Ketones						
2-Octanone	Earthy, weedy	1283	81	MS, RI, O, S	$y = 0.2422x + 0.1693$	0.9947
2-Nonanone	Fresh, green weedy	1386	27	MS, RI, O, S	$y = 0.4332x + 0.2004$	0.9922
2,3-Dihydro-3,5-dihydroxy-6-methyl-4H-pyran-4-one	Sweet, caramellic	2240	9	MS, RI, O	–	–
2-Heptanone	Fruity, sweet	1190	9	MS, RI, O	–	–
2-Decanone	Orange, floral, fatty	1496	9	MS, RI, O	–	–
Alcohols						
1-Octen-3-ol	Mushroom	1459	27	MS, RI, O, S	$y = 0.2412x + 0.1971$	0.9975
Benzyl alcohol	Floral rose	1861	3	MS, RI, O	–	–
N-containing compounds						
Trimethylamine	Fishy	–	729	MS, RI, O, S	–	–
2-Acetyl-1-pyrroline	Popcorn	1317	27	MS, RI, O, S	$y = 0.0585x + 0.7328$	0.9922

Odour description was obtained at the sniffing port.
Identification methods: MS – mass spectra, RI – retention index, O – olfactometry, S – standard compounds.
Calibration equations: y – peak area relative to that of internal standard (nonanoic acid methyl ester), x – content of sample relative to that of the internal standard.
FD – flavour dilution factor, R^2 – coefficient of determination, which reflects the degree to which the regression model fits the observed data.

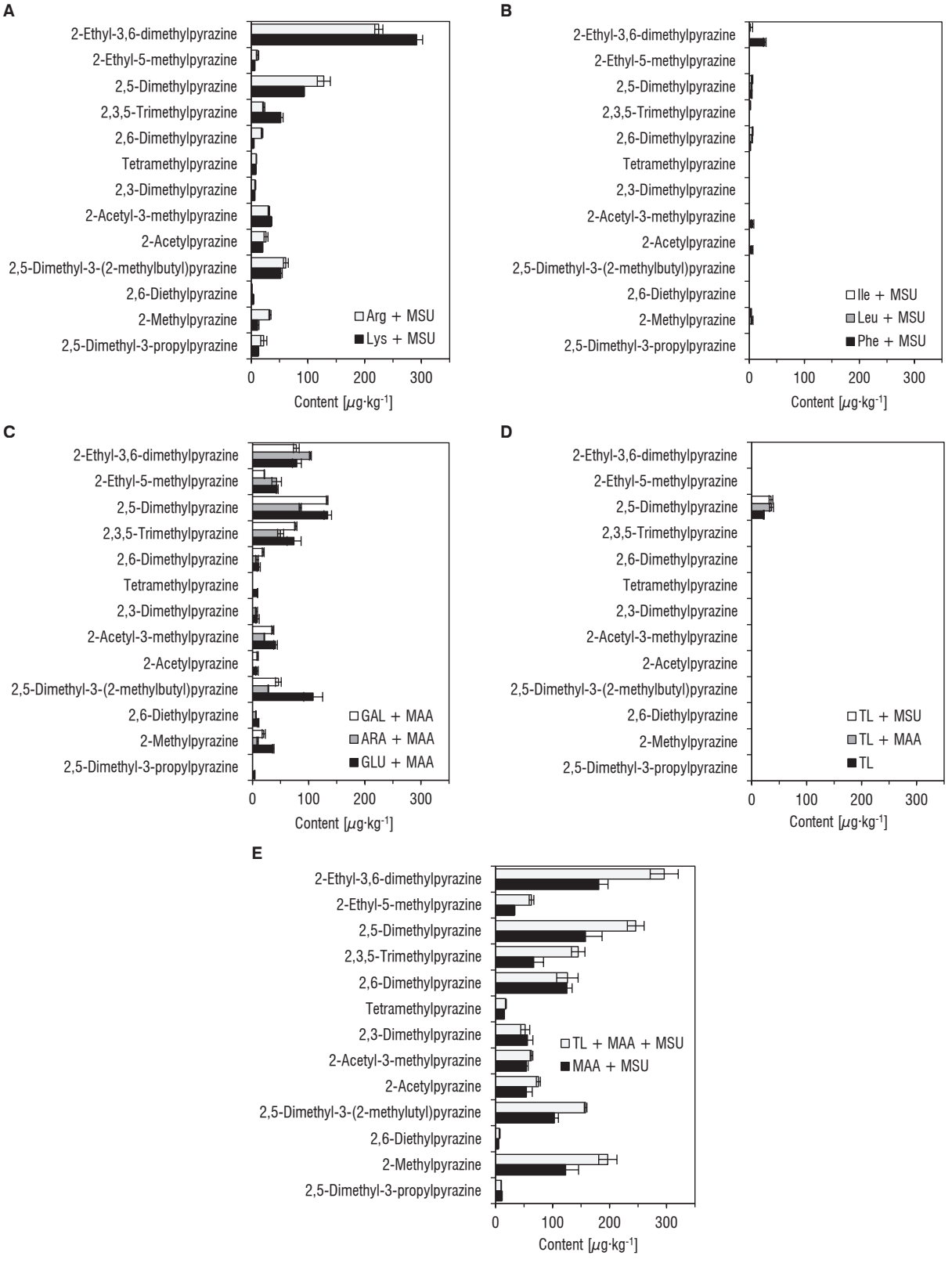

Fig. 1. Contents of pyrazine aroma-active compounds in the various models.

A – Maillard reaction models of Lys or Arg with mixed sugar, B – Maillard reaction models of Phe, Ile or Leu with mixed sugar, C – Maillard reaction models of glucose, galactose or arabinose with mixed amino acid, D – blank model of mixed amino acid or mixed sugar with total lipid, and lipid oxidation model, E – Maillard reaction model of mixed amino acid with mixed sugar, and interaction reaction model.
MAA – mixed amino acid, MSU – mixed sugar, TL – total lipid, GLU – D-glucose, GAL – D-galactose, ARA – D-arabinose.

tively. Only 5 pyrazine AAC were identified in the Maillard reaction models of Phe with mixed sugar (Phe + MSU), Leu with mixed sugar (Leu + MSU) and in Ile with mixed sugar (Ile + MSU), which were 2,5-dimethylpyrazine, 2,6-dimethylpyrazine, 2-acetyl-3-methylpyrazine, 2-ethyl-3,6-dimethylpyrazine and 2-acetylpyrazine, with total contents of 35 ± 7.4 $\mu g \cdot kg^{-1}$, 13 ± 3.3 $\mu g \cdot kg^{-1}$ and 18 ± 3.3 $\mu g \cdot kg^{-1}$, respectively. The types and content of pyrazines were significantly higher in the Lys + MSU and the Arg + MSU models than in the other three models (Phe + MSU, Leu + MSU and Ile + MSU), suggesting a strong dependence of pyrazines formation on the type of amino acid. Such selective AAC enhancement indicates that Lys and Arg play a more important role than Phe, Leu and Ile in forming pyrazine AAC in dried shrimp. This outcome infers that Lys and Arg are the primary amino precursors for these AAC. This is consistent with reports that pyrazine levels increased when Lys and Arg were added to raw shrimps before drying [6]. The molecular structures of amino acids could be a significant determining factor for the rate of Maillard reaction. Lys has one more non-ionized amino group, which could readily catalyse the sugar fragmentation to precede the Strecker degradation and contribute to generation of pyrazines [16]. GENG et al. [27] reported that Arg plays a crucial role in the Maillard reaction in dried squid meat. Lys and Arg contain more than one nitrogen atom and provide a weakly alkaline environment, which can contribute to the formation of pyrazines [28].

In the SSU + MAA models (Fig. 1C), the type and content of pyrazine formed did not strongly correlate with the sugar type. However, their contribution to pyrazine AAC formation was inconsistent among the sugars involved. The largest number of pyrazine species and levels were detected in the Maillard reaction models of GLU with mixed amino acid (GLU + MAA). Here, 13 entities with a total content of 569 ± 60.0 $\mu g \cdot kg^{-1}$ were 1.57 and 1.30 times higher than those of the Maillard reaction models of ARA with mixed amino acid (ARA + MAA) and GAL with mixed amino acid (GAL + MAA), respectively. Therefore, glucose was identified as the substantial carbon-based contributor to pyrazine formation in dried shrimp. Most of the pyrazine AAC were generated in dried shrimp by the Maillard reaction involving Lys, Arg and GLU.

In the TL model (Fig. 1D), only 2,5-dimethylpyrazine was detected, possibly due to a trace amount of amino acid and sugar residuals that remained after the lipid extraction procedure. In the blank model of mixed amino acid with total lipid and mixed sugar with total lipid (TL + MAA and TL + MSU), the content of 2,5-dimethylpyrazine did not increase significantly, so TL could not produce pyrazine with MAA or MSU.

In the interaction model (TL + MAA + MSU, Fig. 1E), the total pyrazine content significantly increased 1.48-fold compared with the MAA + MSU models, but the total number of detected pyrazines only increased by 2 types. Among them, 2,3,5-trimethylpyrazine, 2,5-dimethylpyrazine and 2-ethyl-3,6-dimethylpyrazine had the highest content. Lipids also undergo chemical reaction to form aroma-active compounds during the Maillard reaction [29]. The data suggest a hypothesis that pyrazines in the dried shrimps are produced through Maillard reaction between GLU and Lys or Arg, with lipids mainly playing a role in augmenting the reaction.

Aldehydes

Aldehydes have a low odour threshold and are essential aroma-active compounds in dried shrimp products [22, 30]. A total of five aldehyde AAC were identified in dried shrimp, namely, benzaldehyde, 3-methylbutyraldehyde, 2-methylbutyraldehyde, hexanal and pentanal. Aldehydes are produced from lipids and by the Strecker reaction of amino acids [30, 31]. Aldehydes produced by these two pathways were readily observed in the TL and MAA + MSU models (Fig. 2D, 2E).

Benzaldehyde and 3-methylbutanal were identified in the Phe and Leu models (Fig. 2F). These compounds provide almond and chocolate notes and are commonly detected in processed meat products [32, 33]. In the Phe + MSU and Leu + MSU models (Fig. 2B), the contents of benzaldehyde and 3-methylbutanal were significantly increased by 4.80 and 12.12 times compared with the Phe and Leu models, respectively. Although a single amino acid could generate the corresponding aldehydes under heating, the reaction between amino acids and sugars could further increase the contents of these aldehydes. In the Ile + MSU model, the aldehyde with the highest content was 2-methylbutanal (231 ± 22.1 $\mu g \cdot kg^{-1}$), being formed by the Strecker degradation of Ile [34]. In the SSU + MAA models (Fig. 2C), the content of benzaldehyde was the highest in the ARA + MAA model, while the contents of 3-methylbutanal and 2-methylbutanal were the highest in the GLU + MAA model. Aldehydes were not detected in the Lys + MSU and Arg + MSU models (Fig. 2A), possibly due to no production or degradation reactions [35].

In the TL model (Fig. 2D), some aldehydes from thermal degradation of lipids were detected.

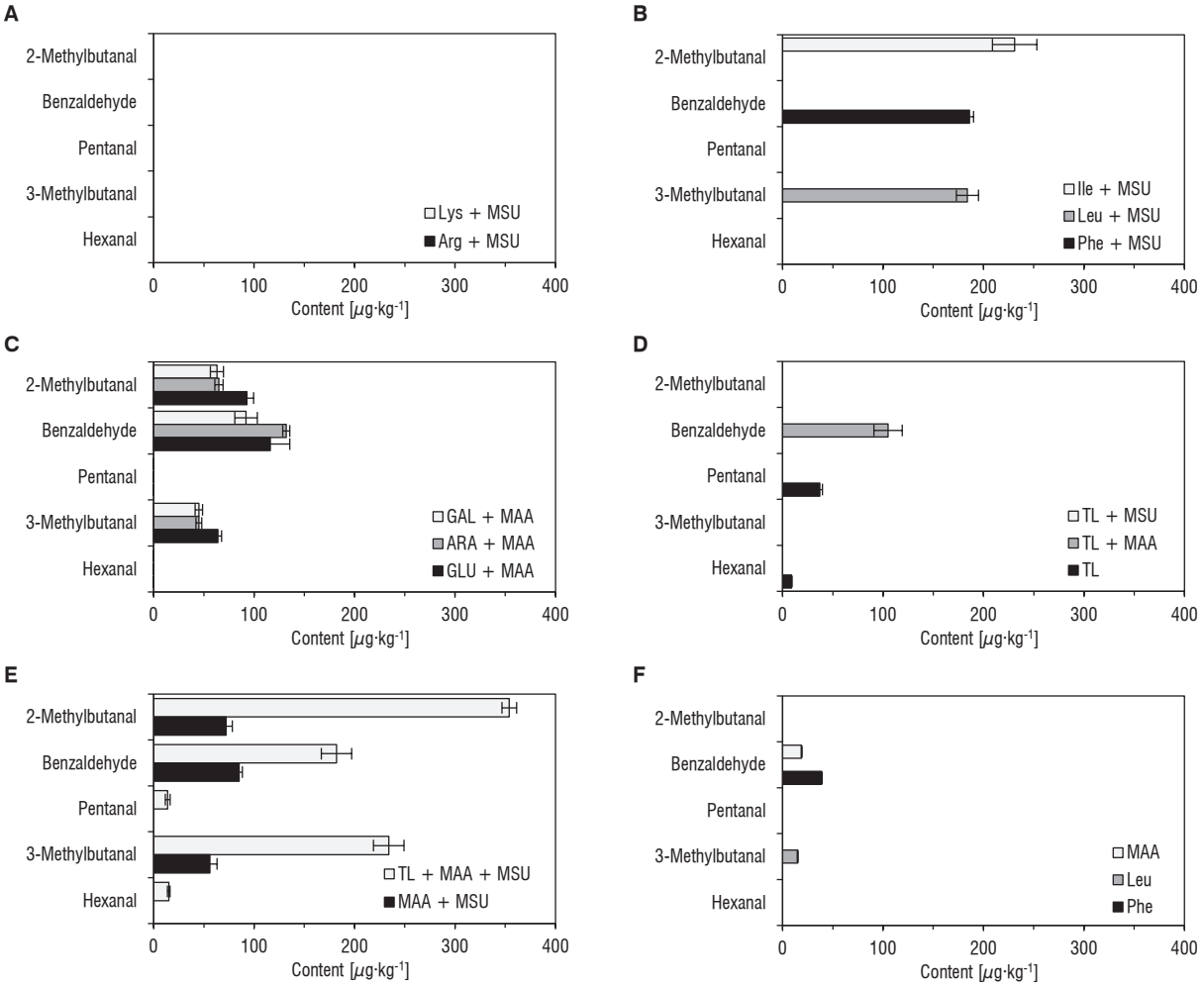

Fig. 2. Contents of aldehyde aroma-active compounds in the various models.

A – Maillard reaction models of Lys or Arg with mixed sugar, B – Maillard reaction models of Phe, Ile or Leu with mixed sugar, C – Maillard reaction models of glucose, galactose or arabinose with mixed amino acid, D – blank model of mixed amino acid or mixed sugar with total lipid, and lipid oxidation model, E – Maillard reaction model of mixed amino acid with mixed sugar, and interaction reaction model, F – blank model of Leu, Phe and mixed amino acid.
MAA – mixed amino acid, MSU – mixed sugar, TL – total lipid, GLU – D-glucose, GAL – D-galactose, ARA – D-arabinose.

Pentanal and hexanal were important aroma-active ingredients detected in the dried shrimps, mainly providing fruity and grassy aroma. Hexanal is derived from oleic acid autooxidation [18, 36]. Pentanal was previously found to be the most abundant aldehyde in boiled shrimps, and its formation was related to the thermal decomposition of linoleic acid hydroperoxide [22]. However, the TL + MAA and TL + MSU models did not contain these two aldehydes. Compared to the MAA + MSU model (Fig. 2E), Strecker aldehyde contents significantly increased by 3.61 times in the TL + MAA + MSU model, indicating that TL promoted the formation of these aldehydes. Combined with these results, Phe, Leu and Ile were the amino acid precursors for benzaldehyde, 3-methylbutanal and 2-methylbutanal, respectively. GLU, GAL and ARA were their carbonyl precursors, but GLU contributed the most to the aldehyde formation. Lipids were the precursor for pentanal and hexanal, promoting the formation of Strecker aldehydes.

Ketones

Five ketone AAC were detected using GC-O analysis in dried shrimp, including 2-octanone, 2-nonanone, 2-heptanone, 2-decanone and 2,3-dihydro-3,5-dihydroxy-6-methyl-4H-pyran-4-one. Their *FD* factors were small. Ketones are products of lipids oxidation [37]. Four ketones were identified in the TL model (Fig. 3D). Among them, 2-octanone and 2-heptanone were

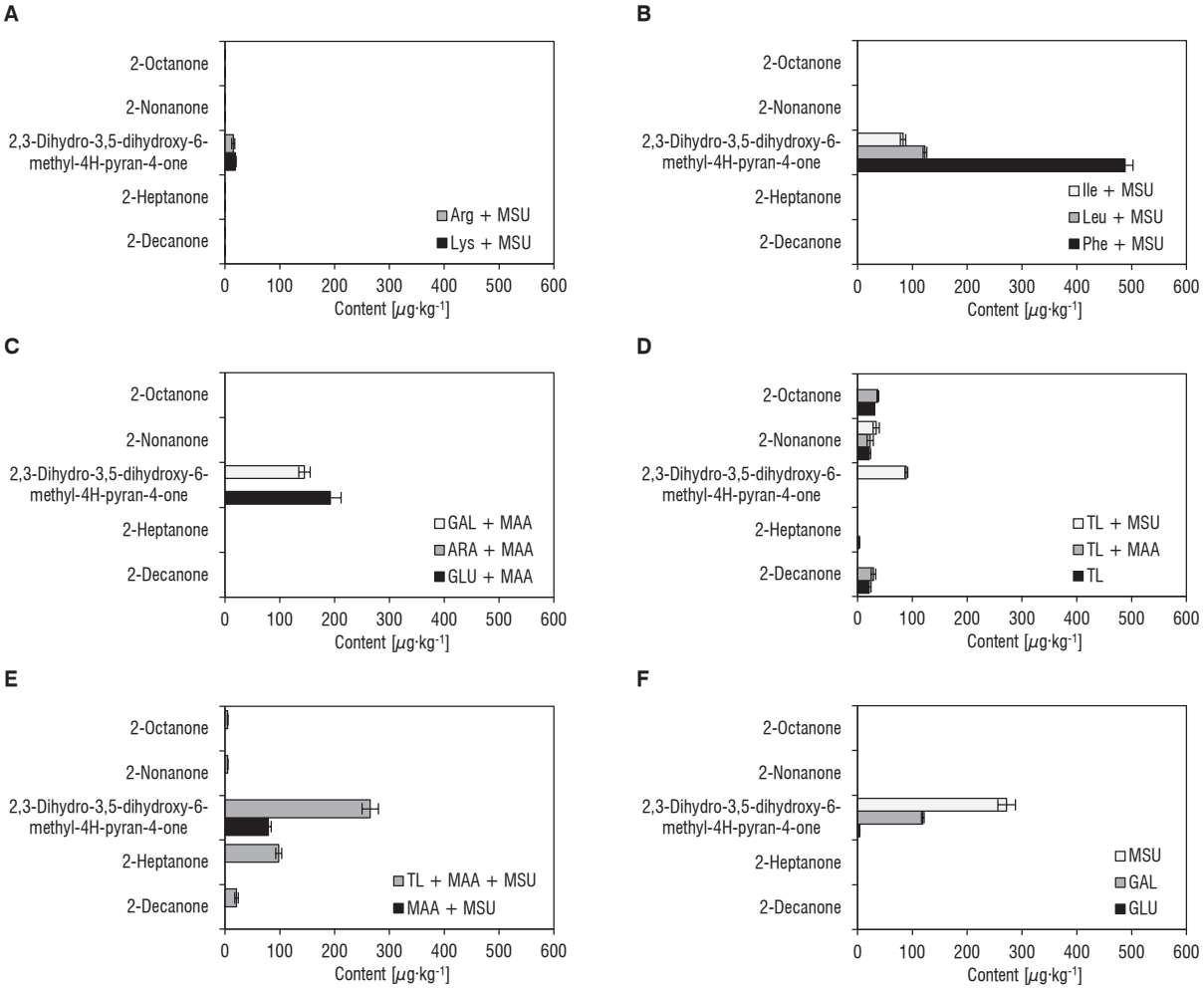

Fig. 3. Contents of ketone aroma-active compounds in the various models.

A – Maillard reaction models of Lys or Arg with mixed sugar, B – Maillard reaction models of Phe, Ile or Leu with mixed sugar, C – Maillard reaction models of glucose, galactose or arabinose with mixed amino acid, D – blank model of mixed amino acid or mixed sugar with total lipid, and lipid oxidation model, E – Maillard reaction model of mixed amino acid with mixed sugar, and interaction reaction model, F – blank model of glucose, galactose and mixed sugar.
MAA – mixed amino acid, MSU – mixed sugar, TL – total lipid, GLU – D-glucose, GAL – D-galactose, ARA – D-arabinose.

previously reported as AAC in shrimps with green, grassy, vegetable and fruity notes [18]. Their formation follows the pathway where fatty acids are first oxidized into α-ketoacids in the process of β-oxidation, which are further decarboxylated to their corresponding methyl ketones with one carbon atom less. 2,3-Dihydro-3,5-dihydroxy-6-methyl-4H-pyran-4-one was identified in the SSU, SSU + MAA and MSU models (Fig. 3A, 3B, 3C, 3D, 3E and 3F). It is formed during caramelization from the sugar skeleton by degradation [38].

Alcohols

Alcohols are generally considered to contribute little to flavour because of their high odour thresholds [30]. Additionally, only few types of alcohols were detected in dried shrimp and they were present at low content. 1-Octen-3-ol, an AAC in the dried shrimps, was only identified in the TL model (Fig. 4D). This alcohol has strong grassy, mushroom and fatty odours, and was found widely in aquatic products [39]. It is primarily produced by oxidizing linoleic and arachidonic acids. Therefore, lipids were the precursor of 1-octen-3-ol.

N-containing compounds

Trimethylamine, a substance widely occuring in fish, is used to indicate the freshness of aquatic products. During the thermal processing of aquatic products, the content of trimethylamine gradually increases due to the thermal decomposition of choline, betaine, methionine or trimethylamine

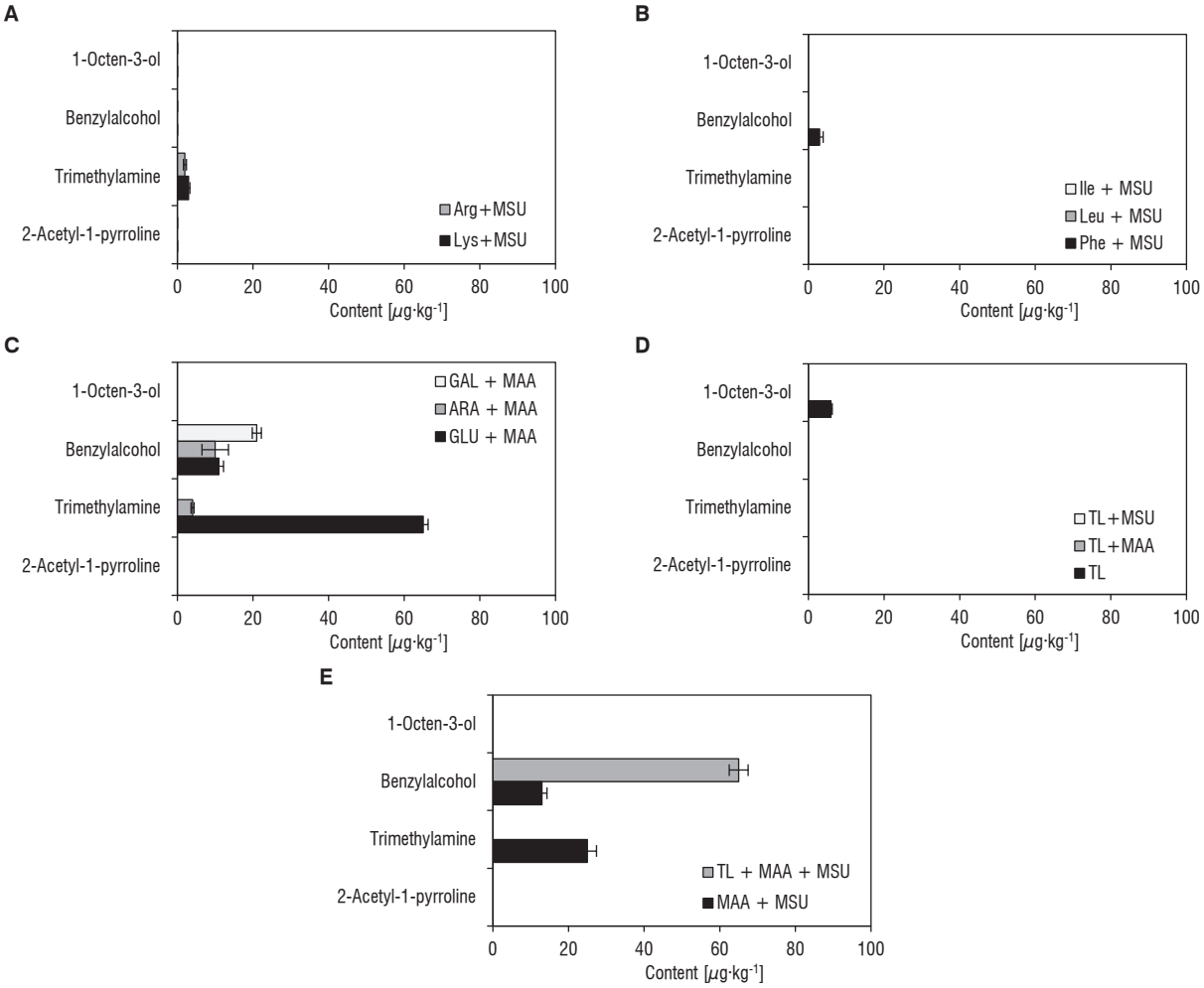

Fig. 4. Contents of alcohols and N-containing aroma-active compounds in the various models.

A – Maillard reaction models of Lys or Arg with mixed sugar, B – Maillard reaction models of Phe, Ile or Leu with mixed sugar, C – Maillard reaction models of glucose, galactose or arabinose with mixed amino acid, D – blank model of mixed amino acid or mixed sugar with total lipid, and lipid oxidation model, E – Maillard reaction model of mixed amino acid with mixed sugar, and interaction reaction model.
MAA – mixed amino acid, MSU – mixed sugar, TL – total lipid, GLU – D-glucose, GAL – D-galactose, ARA – D-arabinose.

oxide. In this study, trimethylamine, an AAC with an *FD* factor of 729 with fishy and grassy notes, was detected in the Arg + MSU and Lys + MSU models (Fig. 4A). A previous study found that adding Lys and Arg to raw shrimps significantly increased trimethylamine levels in dried shrimps and produced dimethylamine, a compound similar to trimethylamine [16].

2-Acetyl-1-pyrroline was another N-containing AAC detected in dried shrimp. It is well-known as one of the key volatile aroma-active compounds associated with popcorn or nutty aroma. However, it could not be detected in all constructed models. The compound is compound derived from the Maillard reaction, degrades rapidly after baking and can be oxidized to 2-acetylpyrrole. 2-Acetylpyrrole was detected in Leu + MSU, Ile + MSU and Arg + MSU models (Tab. S2 in supplementary data).

CONCLUSIONS

A total of 27 AAC were identified using AEDA in dried shrimp, including 13 pyrazines, 5 aldehydes, 5 ketones, 2 alcohols and 2 N-containing compounds, their *FD* factors ranging from 3 to 729. Among them, the *FD* factors of 2-ethyl-3,6-dimethylpyrazine, 2-ethyl-5-methylpyrazine, 2,5-dimethylpyrazine, 2,3,5-trimethylpyrazine, 2,6-dimethylpyrazine and trimethylamine were greater than 243, which means that

they were the most significant AAC of dried shrimp. The relationship between the aroma precursors of dried shrimp and the AAC was tracked intuitively in the constructed models. Lys and Arg were the major amino precursors of 13 pyrazine AAC and trimethylamine. Phe, Leu and Ile were the amino precursors for benzaldehyde, 3-methylbutanal and 2-methylbutanal, respectively. The largest contributor to forming the above AAC was GLU, followed by ARA, and the smallest was GAL. TL was a crucial precursor in forming hexanal, pentanal, 2-octanone, 2-nonanone, 2-heptanone, 2-decanone and 1-octen-3-ol. It also promoted the formation of pyrazines and Strecker aldehyde AAC. This study provides a reference for improving flavour production and regulation of dried shrimp products, in particular the shrimp seasoning.

Acknowledgements

This research was supported by the National Natural Science Foundation of China (32072340), China Agriculture Research System (CARS-48), the Guangdong Seafood Green Processing Technology Innovation and Research Team (2019KCXTD011).

Supplementary data

Supplementary data related to this article can be found at https://www.vup.sk/en/download.php?bulID=2232.

REFERENCES

1. Wang, X. – Liu, B. – Gao, X. – Wang, X. – Li, H. – Xu, L. – Wang, G. – Zhao, K. – Huang, B.: The effects of different UVA photoperiods on the growth performance, immune responses, antioxidant status and apoptosis-related gene expression of the pacific white shrimp (*Penaeus vannamei*). Antibiotics, *11*, 2021, article 37. DOI: 10.3390/antibiotics11010037.
2. Nagarajan, M. – Rajasekaran, B. – Benjakul, S. – Venkatachalam, K.: Influence of chitosan-gelatin edible coating incorporated with longkong pericarp extract on refrigerated black tiger Shrimp (*Penaeus monodon*). Current Research in Food Science, *4*, 2021, pp. 345–353. DOI: 10.1016/j.crfs.2021.05.003.
3. Mall, V. – Schieberle, P.: Evaluation of key aroma compounds in processed prawns (whiteleg shrimp) by quantitation and aroma recombination experiments. Journal of Agricultural and Food Chemistry, *65*, 2017, pp. 2776–2783. DOI: 10.1021/acs.jafc.7b00636.
4. Segura-Borrego, M. P. – Rios-Reina, R. – Ubeda, C. – Callejon, R. M. – Morales, M. L.: Comparison of the novel thin film-solid phase microextraction and sorptive extraction methods for *Picual* and *Hojiblanca* olive oil volatile fraction analysis in headspace. Foods, *9*, 2020, article 748. DOI: 10.3390/foods9060748.
5. Clarke, H. J. – O'Sullivan, M. G. – Kerry, J. P. – Kilcawley, K. N.: Correlating volatile lipid oxidation compounds with consumer sensory data in dairy based powders during storage. Antioxidants, *9*, 2020, acticle 338. DOI: 10.3390/antiox9040338.
6. Zhang, Z. – Ji, H. – Zhang, D. – Liu, S. – Zheng, X.: The role of amino acids in the formation of aroma-active compounds during shrimp hot air drying by GC-MS and GC-IMS. Foods, *11*, 2022, article 3264. DOI: 10.3390/foods11203264.
7. Shi, Y. – Zhu, Y. – Ma, W. – Lin, Z. – Lv, H.: Characterisation of the volatile compounds profile of Chinese pan-fried green tea in comparison with baked green tea, steamed green tea, and sun-dried green tea using approaches of molecular sensory science. Current Research in Food Science, *5*, 2022, pp. 1098–1107. DOI: 10.1016/j.crfs.2022.06.012.
8. Ni, Z.-J. – Wei, C.-K. – Zheng, A.-R. – Thakur, K. – Zhang, J.-G. – Wei, Z.-J.: Analysis of key precursor peptides and flavour components of flaxseed derived Maillard reaction products based on iBAQ mass spectrometry and molecular sensory science. Food Chemistry: X, *13*, 2022, article 100224. DOI: 10.1016/j.fochx.2022.100224.
9. Wang, S.-L. – Lin, S.-Y. – Du, H.-T. – Qin, L, – Lei, L.-M. – Chen, D.: An insight by molecular sensory science approaches to contributions and variations of the key odorants in shiitake mushrooms. Foods, *10*, 2020, article 622. DOI: 10.3390/foods10030622.
10. Avilés-Ramirez, C. – Vioque Amor, M. – Polvillo Polo, O. – Horcada, A. – Gómez-Cortés, P. – de la Fuente, M. Á. – Núñez-Sánchez, N. – Martinez Marin, A. L.: Influence of dietary algae meal on lipid oxidation and volatile profile of meat from lambs with competent reticular groove reflex. Foods, *11*, 2022, article 2193. DOI: 10.3390/foods11152193.
11. Guo, X. – Lu, S. – Wang, Y. – Dong, J. – Ji, H. – Wang, Q.: Correlations among flavor compounds, lipid oxidation indices, and endogenous enzyme activity during the processing of Xinjiang dry-cured mutton ham. Journal of Food Processing and Preservation, *43*, 2019, article e14199. DOI: 10.1111/jfpp.14199.
12. Zhang, D. – Ji, H. – Chen, H. – Liu, S.: Effect of lipids on the aroma attributes of hot-air-dried shrimp (*Penaeus vannamei*). Food and Fermentation Industries, *47*, 2021, pp. 189–196. DOI: 10.13995/j.cnki.11-1802/ts.025553.
13. Chansataporn, W. – Prathumars, P. – Nopharatana, M. – Siriwattanayotin, S. – Tangduangdee, C.: Kinetics of Maillard reaction in a chicken meat model system using a multiresponses modeling approach. International Journal of Chemical Kinetics, *51*, 2019, pp. 14–27. DOI: 10.1002/kin.21224.
14. Alim, A. – Song, H. – Liu, Y. – Zou, T. – Zhang, Y. – Zhang, S. – Raza, A.: Research of beef-meaty aroma compounds from yeast extract using carbon module labeling (CAMOLA) technique. LWT – Food Science and Technology, *112*, 2019, article 108239. DOI: 10.1016/j.lwt.2019.06.006.
15. Zhao, J. – Wang, T. – Xie, J. – Xiao, Q. – Cheng, J. – Chen, F. – Wang, S. – Sun, B.: Formation mecha-

nism of aroma compounds in a glutathione-glucose reaction with fat or oxidized fat. Food Chemistry, *270*, 2019, pp. 436–444. DOI: 10.1016/j.foodchem.2018.07.106.
16. Yu, H. – Seow, Y. X. – Ong, P. K. – Zhou, W.: Effects of high-intensity ultrasound on Maillard reaction in a model system of D-xylose and L-lysine. Ultrasonics Sonochemistry, *34*, 2017, pp. 154–163. DOI: 10.1016/j.ultsonch.2016.05.034.
17. Hwang, H. I. – Hartman, T. G. – Rosen, R. T. – Lech, J. – Chi-Tang, H.: Formation of pyrazines from the Maillard reaction of glucose and lysine-α-amine-15N. Journal of Agricultural and Food Chemistry, *42*, 1994, pp. 1000–1004. DOI: 10.1021/jf00040a031.
18. Zhang, D. – Ji, H. – Liu, S. – Gao, J.: Similarity of aroma attributes in hot-air-dried shrimp (*Penaeus vannamei*) and its different parts using sensory analysis and GC-MS. Food Research International, *137*, 2020, article 109517. DOI: 10.1016/j.foodres.2020.109517.
19. Folch, J. – Lees, M. – Sloane, G. H.: A simple method for the isolation and purification of total lipids from animal tissues. Journal of Biological Chemistry, *226*, 1957, pp. 497–509. DOI: 10.1016/S0021-9258(18)64849-5.
20. Chen, C. – Liu, Z. – Yu, H. – Xu, Z. – Tian, H.: Flavoromic determination of lactones in cheddar cheese by GC-MS-olfactometry, aroma extract dilution analysis, aroma recombination and omission analysis. Food Chemistry, *368*, 2022, article 130736. DOI: 10.1016/j.foodchem.2021.130736.
21. Wang, J. – Yang, Z. J. – Xu, L. Y. – Wang, B. – Zhang, J. H. – Li, B. Z. – Cao, Y. P. – Tan, L.: Key aroma compounds identified in Cheddar cheese with different ripening times by aroma extract dilution analysis, odor activity value, aroma recombination, and omission. Journal of Dairy Science, *104*, 2021, pp. 1576–1590. DOI: 10.3168/jds.2020-18757.
22. Hu, M. Y. – Wang, S. Y. – Liu, Q. – Cao, R. – Xue, Y.: Flavor profile of dried shrimp at different processing stages. LWT – Food Science and Technology, *146*, 2021, article 111403. DOI: 10.1016/j.lwt.2021.111403.
23. Sun, W. – Ji, H. – Zhang, D. – Zhang, Z. – Liu, S. – Song, W.: Evaluation of aroma characteristics of dried shrimp (*Litopenaeus vannamei*) prepared by five different procedures. Foods, *11*, 2022, article 3532. DOI: 10.3390/foods11213532.
24. Hoda, H. M. – Shereen, N. – Mohsen, M. – Manal, G. – Sahar, Y.: Nutty-like flavor production by *Corynbacterium glutamicum* 1220T from enzymatic soybean hydrolysate. Effect of encapsulation and storage on the nutty flavoring quality. Journal of Advanced Research, *10*, 2018, pp. 31–38. DOI: 10.1016/j.jare.2018.01.003.
25. Haider Shipar, M. A.: Formation of pyrazines in dihydroxyacetone and glycine Maillard reaction: A computational study. Food Chemistry, *98*, 2006, pp. 403–415. DOI: 10.1016/j.foodchem.2005.04.023.
26. Yu, H. – Zhang, R. Y. – Yang, F. W. – Xie, Y. F. – Guo, Y. H. – Yao, W. R. – Zhou, W. B. A.: Control strategies of pyrazines generation from Maillard reaction. Trends in Food Science and Technology, *112*, 2021, pp. 795–807. DOI: 10.1016/j.tifs.2021.04.028.
27. Geng, J.-T. – Takahashi, K. – Kaido, T. – Kasukawa, M. – Okazaki, E. – Osako, K.: Relationship among pH, generation of free amino acids, and Maillard browning of dried Japanese common squid *Todarodes pacificus* meat. Food Chemistry, *283*, 2019, pp. 324–330. DOI: 10.1016/j.foodchem.2019.01.056.
28. Cao, J. – Yan, H. – Liu, L.: Optimized preparation and antioxidant activity of glucose-lysine Maillard reaction products. LWT – Food Science and Technology, *161*, 2022, article 113343. DOI: 10.1016/j.lwt.2022.113343.
29. Guo, D. – Wan, P. – Liu, J. – Chen, D. W.: Use of egg yolk phospholipids to boost the generation of the key odorants as well as maintain a lower level of acrylamide for vacuum fried French fries. Food Control, *121*, 2021, article 107592. DOI: 10.1016/j.foodcont.2020.107592.
30. Gu, S.-Q. – Wang, X.-C. – Tao, N.-P. – Wu, N.: Characterization of volatile compounds in different edible parts of steamed Chinese mitten crab (*Eriocheir sinensis*). Food Research International, *54*, 2013, pp. 81–92. DOI: 10.1016/j.foodres.2013.05.018.
31. Shahidi, F. – Hossain, A.: Role of lipids in food flavor generation. Molecules, *27*, 2022, article 5014. DOI: 10.3390/molecules27155014.
32. Wang, Z. – Xu, Z. – Sun, L. – Dong, L. – Wang, Z. – Du, M.: Dynamics of microbial communities, texture and flavor in *Suan zuo yu* during fermentation. Food Chemistry, *332*, 2020, article 127364. DOI: 10.1016/j.foodchem.2020.127364.
33. Zhu, W. – Luan, H. – Bu, Y. – Li, X. – Li, J. – Ji, G.: Flavor characteristics of shrimp sauces with different fermentation and storage time. LWT – Food Science and Technology, *110*, 2019, pp. 142–151. DOI: 10.1016/j.lwt.2019.04.091.
34. Wietstock, P. C. – Kunz, T. – Methner, F. J.: Relevance of oxygen for the formation of Strecker aldehydes during beer production and storage. Journal of Agricultural and Food Chemistry, *64*, 2016, pp. 8035–8044. DOI: 10.1021/acs.jafc.6b03502.
35. Zamora, R. – Hidalgo, F. J.: The Maillard reaction and lipid oxidation. Lipid Technology, *23*, 2011, pp. 59–62. DOI: 10.1002/lite.201100094.
36. Zang, M. – Wang, L. – Zhang, Z. – Zhang, K. – Li, D. – Li, X. – Wang, S. – Chen, H.: Changes in flavour compound profiles of precooked pork after reheating (warmed-over flavour) using gas chromatography-olfactometry-mass spectrometry with chromatographic feature extraction. International Journal of Food Science and Technology, *55*, 2019, pp. 978–987. DOI: 10.1111/ijfs.14306.
37. Li, Y. L. – Wang, X. J. – Xue, Y. – Ruan, S. Y. – Zhou, A. Q. – Huang, S. F. – Ma, H. L.: The preparation and identification of characteristic flavour compounds of Maillard reaction products of protein hydrolysate from grass carp (*Ctenopharyngodon idella*) bone. Journal of Food Quality, *2021*, 2021, article ID 8394152. DOI: 10.1155/2021/8394152.
38. Shakoor, A. – Zhang, C. – Xie, J. – Yang, X.: Maillard reaction chemistry in formation of critical intermediates and flavour compounds and their antioxi-

dant properties. Food Chemistry, *393*, 2022, article 133416. DOI: 10.1016/j.foodchem.2022.133416.

39. Li, X. P. – Liu, Y. W. – Wang, Y. Y. – Wang, J. X. – Xu, Y. X. – Yi, S. M. – Zhu, W. H. – Mi, H. B. – Li, T. T. – Li, J. R.: Combined ultrasound and heat pretreatment improve the enzymatic hydrolysis of clam (*Aloididae aloidi*) and the flavor of hydrolysates. Innovative Food Science and Emerging Technologies, *67*, 2021, article 102596. DOI: 10.1016/j.ifset.2020.102596.

Received 22 August 2023; 1st revised 19 December 2023; 2nd revised 25 January 2024; accepted 30 January 2024; published online 11 March 2024.